4.1.1.5 Solar transition region and quiet corona

Klaus Wilhelm

4.1.1.5.1 The transition region

The transition region (TR) is the interface between the solar chromosphere and the low corona. The electron temperature, T_{e}, increases in this region from about 2.5×10^4 K to 6×10^5 K. Despite the detailed observations obtained over the last 40 years, the physical conditions, and even the morphology, of the TR are not yet fully understood. Reconnection – the merging of oppositely directed magnetic fields – is a major energy source in the TR, but the inherent spatial scales are below the resolution of present-day instruments. The observations have mainly to be performed in the vacuum-ultraviolet (VUV) wavelength range, in which most of the multiply charged ions of the TR radiate. This range can only be observed by space instruments outside the Earth's atmosphere (cf., Sect. 4.1.1.3). The observations obtained until 1990 and the models developed are referenced in [g, h]. Some of the main results were:

(1) The line widths are much wider than expected from the prevailing electron temperatures. The temperature, T_{i} of the emitting or absorbing particles (atoms or ions) and the speed of the unresolved non-thermal motion, ξ, result in a line broadening with a Doppler width of

$$\Delta\lambda_D = \frac{\lambda_0}{c_0}\sqrt{\frac{2kT_{\mathrm{i}}}{m_{\mathrm{i}}} + \xi^2} \quad , \tag{1}$$

where λ_0 is the central wavelength of the line, c_0 the speed of light in vacuum, k the Boltzmann constant, and m_{i} the particle mass, cf., [l].

(2) The spatial structure is very inhomogeneous and dominated by the magnetic fields of the chromospheric network. Spicules with chromospheric material pervade the TR as well as the lower corona of the Sun. Macrospicules are observed in coronal holes (CH) (see Sect. 4.1.2.5.4).

(3) Although the TR is very dynamic with many short-lived events and significant plasma flows, an average downflow seen as Doppler red shift of many emission lines persists and is shown in Fig. 1. Hot coronal lines, however, are blue shifted on average.

The spectrum of the quiet-Sun (QS) TR contains thousands of emission lines (cf., Fig. 3 in Sect. 4.1.1.3). Recent line lists are published by [d, c, b, e]. References to radiance spectra are contained in Table 1. A comparison between a full-Sun spectrum and that of cool stars has been made by [06Pet]. A compilation of the line lists in the VUV range published between 1958 and 2001 in given in [q]. The TR is optically thin for most of the spectral lines, but there are exceptions,

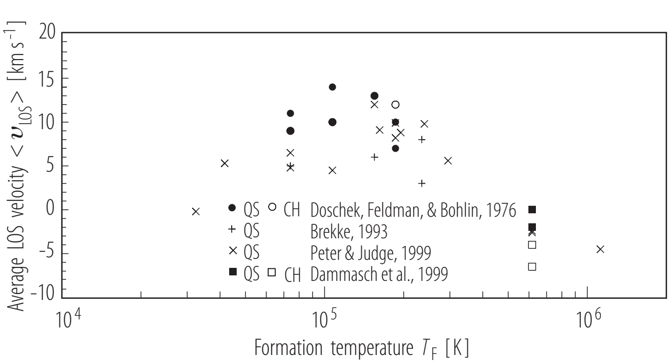

Fig. 1. Average Doppler shifts of VUV emission lines. The line-of-sight (LOS) velocities (positive: red shift, downwards motion) are taken from [76Dos2, 93Bre, 99Pet2, 99Dam]. The largest shifts occur in TR lines at electron temperatures between $\approx 1 \times 10^5$ K and 2×10^5 K.

Table 1. Selected solar radiance and irradiance spectra

Wavelength interval, λ	Data[a]	Origin	Reference
30.8 nm to 38.1 nm	L_λ, Id.	QS	[c]
51.3 nm to 63.3 nm	L_λ, Id.	QS	[c]
46.5 nm to 160.9 nm	L_λ, Id.	corona	[f] [b]
66 nm to 161 nm	L_λ, Id.	corona	[i]
66 nm to 161 nm	L_λ, Id.	QS composite	[04Kre]
117.5 nm to 171 nm	L_λ, Id.	QS, CH, active region	[86San]
120 nm to 900 nm	E_λ		[89Nic]
175 nm to 210 nm	L_λ	Plage	[76Bru]
225.2 nm to 319.6 nm	L_λ, E_λ		[k]
357 nm to 22 μm	L_λ, Id.	Umbra	[03Hin][c]
409 nm to 857 nm	L_λ, E_λ	Calculation	[99Fon]

[a] Id.: Line identification; radiance spectrum: L_λ; irradiance spectrum: E_λ.
[b] An updated version is available from
`http://www.mps.mpg.de/homes/curdt/coronal_atlas.pdf`.
[c] A description of eight solar atlases is given. They can be obtained via
anonymous ftp from `argo.tuc.noao.edu, cd pub/atlas`.

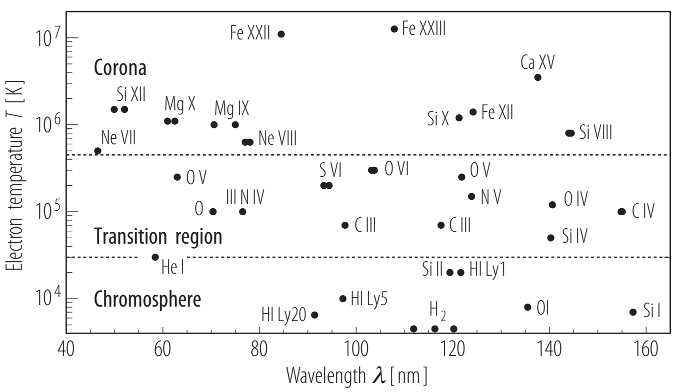

Fig. 2. Strong spectral lines emitted by the solar atmosphere at VUV wavelengths. The approximate electron temperature ranges of the chromosphere, transition region, and corona are indicated as well as the formation temperatures of the lines.

notably H I Lyα. The emission lines provide information on the physical conditions in the TR:
(1) Ratios of radiances of density-sensitive line pairs allow the deduction of electron densities, n_e. The method depends on metastable states of one or both excited ions that can be depopulated by collisions, cf., [69Gab]. Applications gave typical values of $n_e \approx 1 \times 10^{10}$ cm^{-3} for TR plasmas, e.g. [00Lan].
(2) Radiance ratios of temperature-sensitive line pairs can be used to probe electron temperatures. In general, widely separated energy levels of excited states are required in this case, cf., [72Her]. Application of this method by [97Flu, 99Bre, 00Cha] yielded temperatures from 8×10^4 K to 8×10^5 K for TR structures.
(3) The formation temperatures of emission lines also give some indication on the electron temperature of the source regions, cf., e.g. [04Wil]. Prominent emission lines of the solar atmosphere in the VUV wavelength range are shown as wavlength-temperature diagram in Fig. 2.
(4) Line shifts can, in optically-thin plasmas, be interpreted as bulk motions and have been ob-

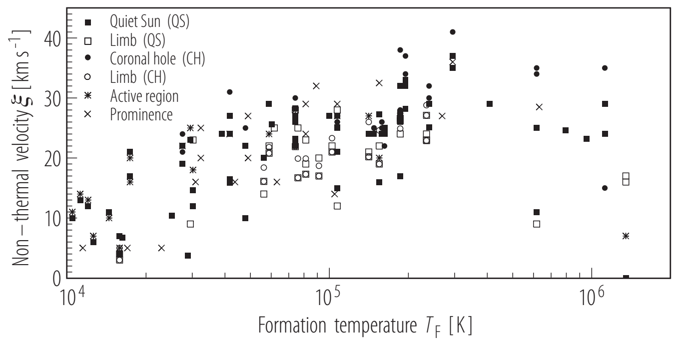

Fig. 3. Non-thermal velocities of ions emitting spectral lines as a function of the formation temperature (data from [75Bol, 76Fel1, 76Dos1, 77Kje, 93Der, 98Cha1, 98deB, 99Pet1, 04Xia, 04Cir, 05Aki]).

served extensively, e.g. [94Bre, 97Bre, 97War1, 98Cha3, 99Gal]. A correlation of red shifts and radiance increases was often observed, cf., [99Pet1, 03Brk].
(5) Based on the assumption $T_i = T_e$, the non-thermal velocities, ξ, in the TR can be evaluated as shown in Fig. 3. At TR temperatures, the highest ξ are between 30 km s^{-1} and 40 km s^{-1}. The decrease towards higher formation temperatures might be caused by core and tail components of the emission line profiles at the TR/corona interface [01Pet].

4.1.1.5.1.1 The magnetic network

The chromospheric network is seen in all TR lines formed between 2.5×10^4 K and $\approx 4 \times 10^5$ K. Typical network structures can be seen in Fig. 4. Observations by [74Ree, 76Fel2] showed that

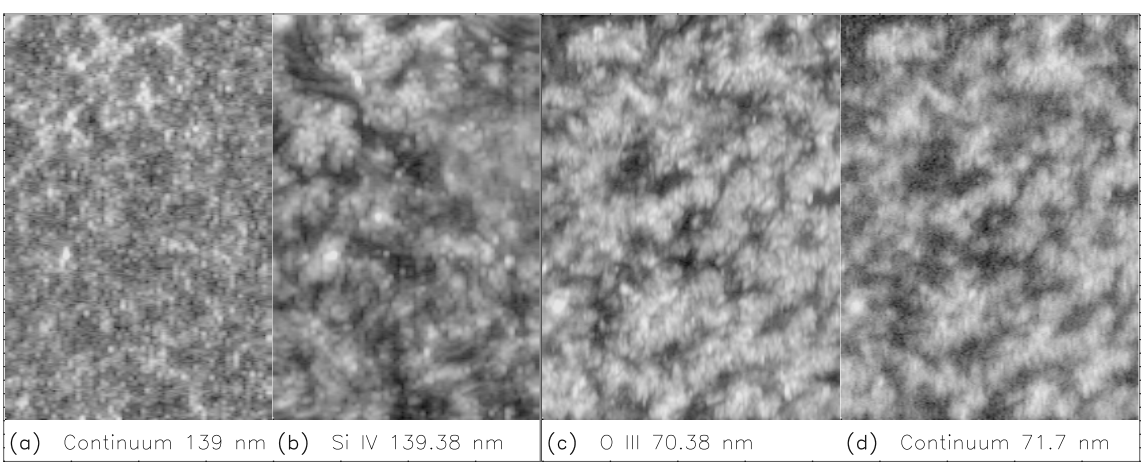

Fig. 4. Structure of the chromospheric network at different formation temperatures (T_F). **a)** The network lanes are composed of small bright dots in the Si I continuum ($\approx$ 7 000 K) at 139 nm (size of area: $\approx$ 144 Mm $\times$ 220 Mm). **b)** At $T_F \approx$ 74 000 K, the formation temperature of the Si IV line at 139.38 nm, the structure of the network lanes (simultaneously recorded with the 139 nm continuum) is much more pronounced. Small loop-like features straddle the lanes and some faint arches are crossing the internetwork regions. **c)** In the O III 70.38 nm line, the general network structure is very similar to that of Si IV, although the formation temperature is about 100 000 K. (The O III and 71.7 nm continuum observations were obtained on the following day) **d)** The structure seen in the H I Lyman continuum at 71.7 nm is very different from that of the Si I continuum.

the contrast between network lanes and cell interiors had a maximum at lines emitted between 1×10^5 K and 2×10^5 K. A 2D model of the chromosphere, TR and corona by [76Gab] placed the primary TR on expanding magnetic flux tubes above the network lanes and a thin secondary TR above the cells. This model was extended by [86Dow]. The network seen on the disk is remarkably similar in QS areas and CHs, but on the limb it has a greater vertical extension in CHs [74Hub, 78Boh, j, 04Wie, 06Mar2]. The width of the average network lane has a minimum of ≈ 4 Mm near 2×10^5 K. At temperatures below 1×10^5 K, the width increases to ≈ 7 Mm [76Fel2, 98Gal]. The electron pressure is nearly constant in the low TR [98Dos]. The occurrence probabilities of the radiance variations of TR lines are normally distributed, if plotted on a logarithmic scale [97Lem, 98Wil1, 99Gri, 04Kre]. The widths of the distribution functions vary with the formation temperature and have a maximum near 1×10^5 K.

The energy required to accelerate the solar wind is believed to stem from reconnection events of entangled magnetic fields in or near the magnetic network leading to explosive events, blinkers, microflares, and other small-scale events [92Axf, 94Mos, 97Inn, 97Har, 02Win, 02Ter].

4.1.1.5.1.2 Explosive events

Explosive events are small-scale, high-velocity phenomena in the TR, see, e.g. [83Bru, 89Der, 94Kje, 94Mos, 97Inn, 01Inn]. Spectral line profiles during the events consist of three Gaussian profiles with one component at rest and the others shifted by ≈ 10 pm to either red or blue [81Der]. Plasma speeds of up to and above 100 km s^{-1} are observed along the line of sight (LOS) with durations of a few minutes. Explosive events are caused by magnetic field line reconnection [94Der], but are not associated with X-ray bright points (BP) (cf., Sect. 4.1.1.5.2.4) [94Mos]. Cancellations of photospheric magnetic fields are observed in relation to explosive events [91Der, 98Cha2] as well as bi-directional jets [97Inn] and chromospheric upflow events [98Cha3]. The energy release is estimated to be 1×10^{16} J to 1×10^{18} J per event [02Win]. Events observed in the TR at 1.8×10^5 K do, in general, not show a signature in the corona [02Ter].

An electron density of $n_e \approx 7 \times 10^{10}$ cm^{-3} was obtained during an event by [91Der]. Line-ratio studies indicated that there is a density increase by a factor of about three and, in some cases, a significant electron temperature, T_e, enhancement [01Ter, 05Men]. The average size is estimated to be 1.8 Mm with a birth rate of 2500 s^{-1} over the entire Sun. Despite this high rate, the events do not seem to be directly important for the coronal heating process [04Ter].

4.1.1.5.1.3 Blinkers

VUV brightenings identified by [97Har] exhibited radiance enhancements by a factor of two to three in TR lines. The characteristics of these "blinkers" are: (a) an average duration of 13 min, (b) a size ≈ 6 Mm $\times$ 6 Mm, and (c) no significant Doppler broadening [99Har]. No increase was found in the electron density of a short-duration blinker. The line width of O VI nearly reached thermal values at the maximum of a blinker event. The lack of substantial non-thermal velocities and the missing signature of blinkers in the corona are used as arguments for a chromospheric driver of blinkers, [01Brk, 03Pet]. Emissions formed at ≈ 1 MK are co-spatial with H I Hα at $\approx 1 \times 10^4$ K, but not with C IV at 1×10^5 K [03DeP]. Explosive events and blinkers are not directly related [03Har].

4.1.1.5.1.4 Microflares and nanoflares

These features are very small flares (cf., Sect. 4.1.2.7) with very low energy output. They are mentioned here, because they are a common reconnection phenomenon in the magnetic network of the quiet Sun. The distribution of the energy released forms a power law with a slope of $\gamma \approx -1.8$ as determined by [00Asc]. However, [00Par2] found values of $\mid \gamma \mid$ greater than two, which would imply that the smallest events dominate the total flare-generated energy.

4.1.1.5.2 The quiet corona

Above the TR, the solar corona extends to large distances from the Sun. The structural changes of the solar atmosphere from the chromosphere through the TR to the corona can be seen in Fig. 5.

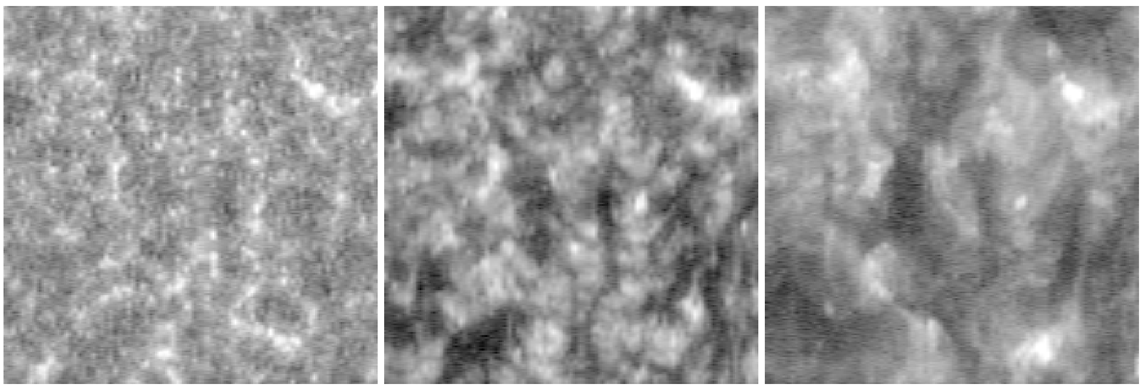

Fig. 5. Structure of the magnetic network in the chromosphere, TR, and corona [02Wil2]. The observations were made in the continuum near 154 nm, in the C IV line at 154.8 nm and the Ne VIII line at 77.0 nm. The size of the area shown is 155 Mm × 155 Mm.

The corona consists of three different components [p, g, h, n]:
(1) The F corona – scattered solar radiation by interplanetary dust.
(2) The K corona – scattered solar radiation by free electrons in the corona.
(3) The L corona – the sum of the coronal emission lines and continua.

The F and K components together are called white-light corona, which can best be seen during solar eclipses (see [07Pas] for recent observations). The F corona shows sharp Fraunhofer lines, whereas the K corona does not, because of the high thermal speeds of the scattering electrons. The K corona is much brighter than the F and L components. The spectrum of the L corona is very complex. The green, yellow, and red lines were identified as emissions from highly-ionized iron and calcium indicating the high temperature of the corona with values of more than 1 MK [37Lyo, 39Gro, 43Edl]. The corona eventually expands and transforms into the solar wind. Two types of the solar wind can be identified: a quasi-stationary fast wind (see Sect. 4.1.1.5.2.3) and a transient slow wind (see Sect. 4.1.1.5.2.6) [91Neu, 97Woc, 98McC].

The spatial structure of the corona is determined by the topology of the magnetic field: open field regions corresponding to dark CHs and closed magnetic fields related to relatively bright areas. Some of the closed loops are extending into so-called “helmet streamers” [97Mos]. Polarization measurements can probe the coronal magnetic field via the Hanle effect [86Sah, 02Rao].

The structure of the corona changes with the solar cycle. Near the minimum, the equatorial latitudes are occupied by closed magnetic regions and the poles by large CHs. During the maximum, the solar corona (cf., Sect. 4.1.2.6) is much more symmetric with many active regions (cf., Sect. 4.1.2.1) in between, see, e.g. [00Syk]. The response of the solar wind to the solar activity cycle is reviewed by [06Mar1].

An atlas of coronal VUV spectra has been compiled by [f]. Logarithmic radiance variations of coronal lines are normally distributed at medium levels and change to a power-law distribution at high radiances [00Ale]. The physics of the solar corona is treated in [a].

4.1.1.5.2.1 Coronal holes

CHs (Koronalöcher) in the solar atmosphere have first been identified by [o] in the green Fe XIV 530.3 nm line. Their low electron density leads to a deficiency in the radiance of coronal emission lines [72Mun]. CHs are visible in the He I and He II lines, but not in most of the other TR lines [73Tou]. CHs are the site of coronal plumes (see Fig. 7 and Subsect. 4.1.1.5.2.5) and the fast solar wind outflow (see Fig. 6 and Subsect. 4.1.1.5.2.3).

An anomalous rotation – a rigid rotation and not a differential one as the photosphere – of large north-south oriented CHs was found [75Tim, 77Boh, 78She, 99Zha]. The CHs can be identified with the M regions introduced by [40Bar]. Low-latitude CHs during the solar maximum have been studied by [04Mir].

4.1.1.5.2.2 Coronal plasma parameters in QS regions and CHs

The electron and the ion temperatures are not the same in the corona [97See, 98Tuc, 99Gol]. Observations demonstrated excessive line broadening of the Mg X lines at 60.9 nm and 62.5 nm above the limb, indicating indeed high ion temperatures [90Has], see also [00Dos, 02Har, 05Wil, 06Zaq].

Near the limb, the electron density is $\approx 2 \times 10^8$ cm^{-3}, decreasing to 6×10^7 cm^{-3} at a height of 70 Mm in CHs [99Flu]. The corresponding temperatures are 7.5×10^5 K and 8.5×10^5 K. The electron density obtained at an altitude of $\approx$ 7 Mm is typically 1×10^8 cm^{-3} and $\approx 5 \times 10^6$ cm^{-3} at 200 Mm height [97Dos, 98Wil2]. At greater altitudes, very high (anisotropic) ion temperatures of much more than 10 MK have been detected by coronagraphs on rockets and spacecraft [80Koh, 99Koh, 06Koh, 99Cra1, 99Ess, 03Fra]. The electron density stratification may have an influence on the observed line width and anisotropy [04Rao]. Because of the rotation of the Sun, tomographical procedures can be used to determine the 3D electron density distribution in the corona [02Fra].

Hydrogen and protons are coupled by charge exchange in CHs at heliocentric distances below 2 $R_\odot$ to 3 $R_\odot$ [82Wit]. With this assumption and using the higher members of the H I Lyman series, [99Mar] found proton temperatures of 2×10^5 K at heights of 18 Mm above the limb, and line-width contributions between 20 km s^{-1} and 40 km s^{-1} from turbulence. H I Lyα observations obtained at greater heights indicate line widths of more than 200 km s^{-1} [97Koh]. Above CHs, bi-Gaussian distributions of H I Lyα, O VI, and Ne VIII profiles with wide wings have been observed by [96Koh, 99Wil].

The interaction of ion-cyclotron waves – generated in the lower atmosphere, for instance, by microflares (cf., Sect. 4.1.1.5.1.4) – with the ions in the CH plasma is one candidate for heating the corona and accelerating the fast solar wind. Observations of the effective temperature show an increase with decreasing values of q/m, the charge-to-mass ratio of the ions, as expected for ion-cyclotron heating [90Has, 98Tuc, 00Ban2, 02Pat].

Electron temperatures smaller than 1 MK – decreasing with height – were found in the corona above a polar CH; much less than in the bright equatorial corona of the QS [98Dav]. The CH plasma is not homogeneous: about 10 % of the gas is hot ($\approx$ 2 MK) and the rest cooler at $\approx 0.8 \times 10^5$ K [77Chi].

CH temperatures can also be estimated from the so-called "freeze-in" temperatures of charge states of ions in the solar wind. A temperature of $\approx$ 1.5 MK was obtained in a CH at 1.4 $R_\odot$ by [97Koy]. However, non-Maxwellian electron velocity distributions with an enhanced supra-thermal tail are required in the inner corona to account for the observed charge distributions [83Owo, m, 03Che].

4.1.1.5.2.3 Fast solar wind outflow

The fast solar wind is emanating on open magnetic field lines from CHs [73Kri]. Direct outflow from the Sun with speeds a little above 10 km s^{-1} was found for Mg^{8+}, Mg^{9+}, and Si^{10+} ions with Doppler observations [76Cus, 77Cus]. Outflows of O^{4+} and Mg^{9+} ions with speeds of 7 km s^{-1} and 12 km s^{-1}, respectively, were observed in CHs, if the remainder of the solar disk is at rest [82Rot, 97War2]. Concentrated outflow of Ne^{7+} ions occurred near the intersections and boundaries of the network [99Has, 99Dam, 04Pop, 05Aio]. The outflow is strongest in the dark regions of CHs [00Wil2, 00Gio, 00Pat, 05Wie, 05Tuc], and could be related to so-called magnetic funnels, in which outflow speeds of ≈ 10 km s^{-1} were observed at a height of ≈ 20 Mm at a temperature of $T_e \approx 600\,000$ K. A small coronal hole and the initial outflow of the solar wind is shown in Fig. 6.

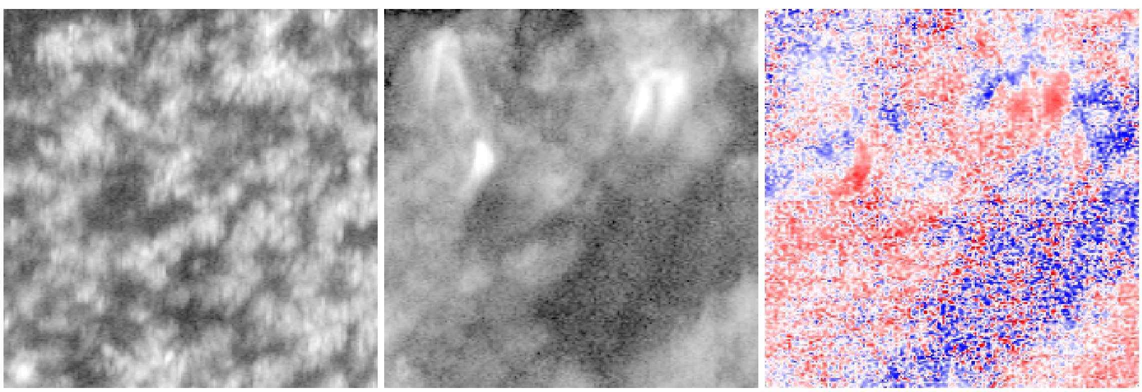

Fig. 6. (see color-picture part, page 614) A small coronal hole seen on the solar disk in the Mg IX (70.6 nm) line (middle panel). In the continuum near 71 nm (on the left) the magnetic network structure is the same inside and outside the coronal hole. The Doppler image shows LOS velocities of ±30 km s^{-1} with outflows (blue shifts) in the hole area.

Doppler dimming is another method for measuring flow speeds in the corona [70Hyd, 82Wit]. It depends on the variation of the resonantly scattered radiation as a function of the flow speed of the plasma relative to the source of the irradiation. The results obtained showed that the acceleration of the fast solar wind to ≈ 400 km s^{-1} occurred within 2 $R_\odot$ [99Cra2]. Speeds of about 70 km s^{-1} can be found in dark regions of polar CHs at altitudes of 35 Mm [00Pat]. These interplume regions are the acceleration areas of the fast solar wind also according to [03Ter], but [03Gab] concluded that the outflow speed in polar plumes was significantly higher than in interplume regions (cf., Sect. 4.1.1.5.2.5). Linear polarization measurements of the O VI line at 103.2 nm by [02Rao] provide constraints on the magnetic field and solar-wind flow in polar CHs.

4.1.1.5.2.4 Bright points

Small bipolar magnetic features in the corona are called BPs [73Tou, 74Gol, 90Gol]. They have a mean lifetime of 8 h in X rays and 20 h in the extreme ultraviolet (EUV) [01Zha]. Radiance variations with time scales of ≈ 6 min were observed in sub-structures of BPs [79She, 81Hab]. In a review of BP observations, [92Hab] emphasizes their arcade structure of loops with different temperatures and emission variations on the time scale of minutes.

Observations by [03Mad] confirmed the results of [93Web, 94Mos] that BPs were related to the cancellation of magnetic flux. Electron densities in BPs range between 1×10^9 cm^{-3} and 1×10^{10} cm^{-3} at formation temperatures of 1.3 MK to 2 MK [05Uga]. Doppler velocities above a BP of ±15 km s^{-1} (He II) and ±35 km s^{-1} (Fe XVI) have been observed by [07Bro]. Although BPs are a signature of coronal activity (cf., Subsect. 4.1.2.6), they are included here, because they are present even at very low solar activity levels.

4.1.1.5.2.5 Coronal plumes

Polar coronal plumes are prominent features of CHs in the visible and at VUV wavelengths in spectral lines with formation temperatures ≤ 1 MK (see Fig. 7) [50Van, 74Boh, 95Fis, 97DeF, 97Koh, 98Wil2, 98Wan, 99Lit]. On the disk, a density of $n_e \simeq 1.2 \times 10^9$ cm^{-3} is typical for a plume, about twice the value of the surrounding CH plasma [03Del]. A density ratio of ≈ 5 between plumes and interplume regions was found by [06Wil], with plume material occupying less

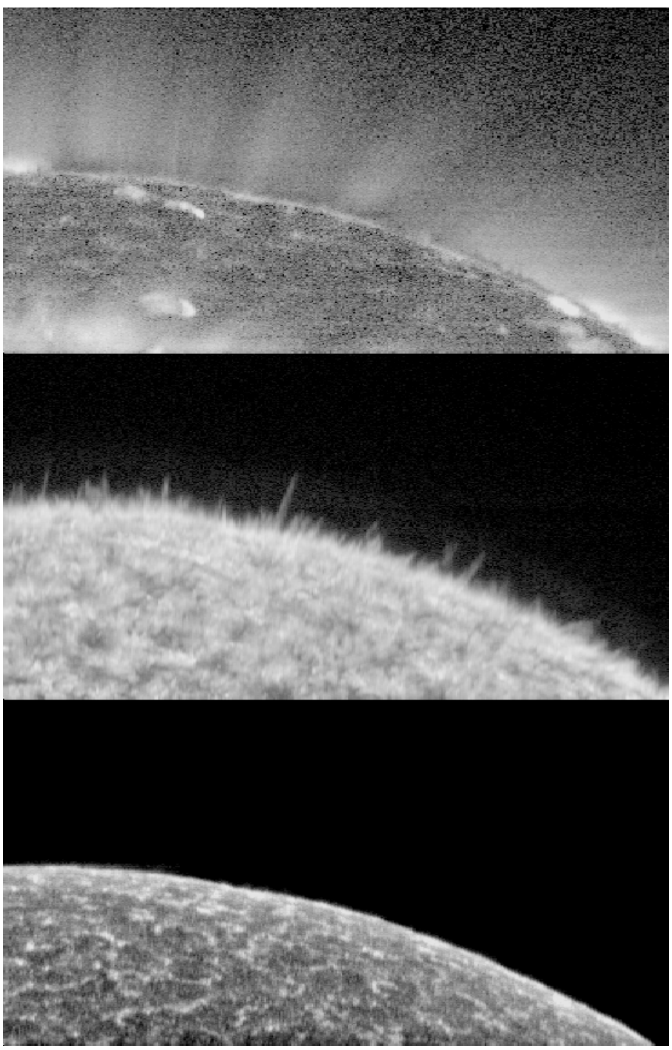

Fig. 7. A section of the north polar cap of the Sun seen in three emission lines with very different formation temperatures from 1.1×10^6 K down to less than 3×10^4 K [00Wil1]. The Mg X line at 62.494 nm (top panel) shows the dark CH region with bright points and some polar coronal plumes on open field lines. Small QS regions were present near the southern edge. The O V (62.973 nm) line in the middle panel is characterized by the chromospheric network and spicule activity. Spicules are absent in the C I (124.941 nm) line in the lower panel, but the network is clearly defined.

than 8 % of the intervening space along the LOS. Coronal plumes are often associated with BPs.

The widths of VUV emission lines are narrower within plumes than outside [95Koh, 97Ant, 97Cor, 97Has, 00Ban2]. Plume structures between 1.1 $R_\odot$ and 3 $R_\odot$ exhibited super-radial expansion and were episodic in nature, lasting $\approx$ 24 h, but recurring at the same location with respect to the Sun [01DeF]. Coronal plumes occur on field lines of the dominant polarity in contact with the minority polarity, but most of the open flux does not carry plume material and, therefore, plumes are not the main source of the fast solar wind [97Wan].

Radiance increases propagate outwards along plumes (with speeds of about 100 km s^{-1}) and recur quasi-periodically on time scales of $\approx$ 10 min [98DeF]. They are interpreted as slow magnetosonic waves by [99Ofm]. Other waves with periods of 10 min to 25 min (and even longer periods in interplume regions) were found by [00Ban1, 01Ban].

The Mg IX line pair at 70.6 nm and 75.0 nm resulted in an electron temperature near 8×10^5 K between polar plumes and even lower values inside plumes [98Wil2]. A Differential Emission Measure (DEM) (cf., [05Lan]) analysis of polar plume peaked at 7.8×10^5 K. A plume in an equatorial CH had very similar temperatures [03Del], but somewhat higher values of $\approx$ 1.0 MK have been reported by [99You]. Plumes are, however, not seen in Fe XII at a formation temperature of 1.4 MK [00Fel]. An increase with height was observed, e.g. by [06Wil].

4.1.1.5.2.6 The equatorial corona, coronal loops, and the slow solar wind

Coronal loops are defining the magnetically-closed corona. There is little temperature variation along the loops [99Len], and filamentation seems to be of importance to maintain a rather constant temperature [00Rea].

Plasma flows in coronal loops were first observed by [78Fou]. Short-lived siphon flows with speeds of 120 km s^{-1} in loops have been seen by [06Doy]. Loops with constant cross-sections are much more typical than those with wider cross section at the top, where temperatures have values of $\approx$ 4 MK, cf., [96Kan]. QS coronal loops with heights of 700 Mm can survive for days. Since the electron density greatly decreases between the base and the top, differential settling of the elements will occur, and iron is by a factor of two to three less abundant relative to neon or silicon at 1.5 $R_\odot$ than near the photosphere [97Ray, 99Fel].

An isothermal electron temperature of 1.3 MK in the equatorial streamer plasma between 1.05 $R_\odot$ and 1.5 $R_\odot$ was found by [97Ray, 99Fel, 00Par1, 02War]. Closer to the limb, an increase of more than 1×10^5 K was measured starting near 1.1 MK. The quiet equatorial corona at low altitudes is cooler ($\approx$ 1 MK) than the corona at mid-latitudes ($\approx$ 1.5 MK). Near the equator high-density ($n_e \approx 5 \times 10^9$ cm^{-3}) TR plasma and low-density ($n_e \approx 2 \times 10^8$ cm^{-3}) coronal plasmas are present at the same height of 5 Mm [02Wil1]. The iron lines Fe IX to Fe XV observed in streamers yielded higher temperatures during the solar maximum ($\Delta T = 0.8$ MK) than under minimum conditions [02Fol]. A quiescent streamer has been studied in detail by [06Uzz], including its elemental abundance. The composition of the solar atmosphere is strongly influenced by the First Ionization Potential (FIP) effect, cf., e.g. [98Fel, 07Fel]. Compared to the photosphere (cf., Sect. 4.1.1.4 "Solar photosphere and chromosphere", see also Fig. 3 of Sect. 4.1.2.1), elements with a FIP bias of less that 10 eV are overabundant in the corona by a factor of about four relative to high-FIP elements, but large variations can occur. A spectrum of the equatorial corona from 50 nm to 161 nm has been observed by [i].

Relatively little is known about the slow solar wind that is originating from closed magnetic regions. Small coronal features tracked by [97She] in the slow solar wind indicate a source at 3 $R_\odot$ and an acceleration of $\approx$ 4 m s^{-1} to a speed of 300 km s^{-1} near 25 $R_\odot$. The outflow providing the mass flux for the slow solar wind starts near the boundaries of closed and open magnetic field regions [97Hab, 97Woo, 02Str, 05Ant].

4.1.1.5.3 References for 4.1.1.5

Catalogues and monographs

a Aschwanden, M.J.: Physics of the Solar Corona. An Introduction with Problems and Solutions, 2nd edition, New York, Berlin: Springer (2005).
b Brekke, P., Brynildsen, N., Kjeldseth-Moe, O., et al.: Adv. Space Res. **26(3)** (2000) 457.
c Brooks, D.H., Fischbacher, G.A., Fludra, A., et al.: Astron. Astrophys. **347** (1999) 277.
d Curdt, W., Feldman, U., Laming, J.M., et al.: Astron. Astrophys. Suppl. Ser. **126** (1997) 281.
e Curdt, W., Brekke, P., Feldman, U., et al.: Astron. Astrophys. **375** (2001) 591.
f Curdt, W., Landi, E., Feldman, U.: Astron. Astrophys. **427** (2004) 1045.
g Durrant, C.J.: Landolt-Börnstein, NS, Vol. VI/2a, Astronomy and Astrophysics (K. Schaifers, H.H. Voigt, eds.), Berlin, Heidelberg, New York: Springer-Verlag (1981) p. 102.
h Durrant, C.J.: Landolt-Börnstein, NS, Vol. VI/3a, Astronomy and Astrophysics (H.H Voigt, ed.), Berlin, Heidelberg, New York: Springer-Verlag (1993) p. 91.
i Feldman, U., Behring, W.E., Curdt, W., et al.: Astrophys. J. Suppl. Ser. **113** (1997) 195.
j Feldman, U., Dammasch, I.E., Wilhelm, K., et al.: Images of the Upper Solar Atmosphere from SUMER on SOHO, ESA SP-**1274**, Noordwijk: ESA Publ. Div. (2003).
k Kohl, J.L., Parkinson, W.H., Zapata, C.A. et al.: Astrophys. J. Suppl. Ser. **44** (1980) 295.
l Mariska, J.T.: The Solar Transition Region, Cambridge: Cambridge University Press (1992).
m Marsch, E.: Physics of the Inner Heliosphere, Vol. **2** (R. Schwenn and E. Marsch, eds.) Berlin etc.: Springer-Verlag, (1991) p. 45.
n Stix, M.: The Sun, 2nd edition, Astronomy and Astrophysics Library, Berlin: Springer-Verlag (2004).
o Waldmeier, M.: Die Sonnenkorona, Basel, Stuttgart: Verlag Birkhäuser (1951).
p Waldmeier, M.: Landolt-Börnstein, NS, Vol. VI/1 (1965) p. 116.
q Wilhelm, K.: J. Atmos. Terr. Sol. Phys. **65** (2003) 167.

Special references

37Lyo Lyot, B.: L'Astronomie **51** (1937) 203.
39Gro Grotrian, W.: Die Naturwissenschaften **27** (1939) 214.
40Bar Bartels, J.: Terr. Magn. Atmos. Electr. **45** (1940) 339.
43Edl Edlén, B.: Zeitschr. Astrophys. **22** (1943) 30.
50Van Van de Hulst, H.C.: Bull. Astron. Inst. Netherland **11** (1950) 135.
69Gab Gabriel, A.H., Jordan, C.: Nature **221** (1969) 947.
70Hyd Hyder, C.L., Lites, B.W.: Sol. Phys. **14** (1970) 147.
72Her Heroux, L., Cohen, M., Malinovsky, M.: Sol. Phys. **23** (1972) 369.
72Mun Munro, R.H., Withbroe, G.L.: Astrophys. J. **176** (1972) 511.
73Kri Krieger, A.S., Timothy, A.F., Roelof, E.C.: Sol. Phys. **29** (1973) 505.
73Tou Tousey, R., Bartoe, J.-D.F., Bohlin, J.D., et al.: Sol. Phys. **33** (1973) 265.
74Boh Bohlin, J.D., Sheeley, N.R., Jr., Tousey, R.: Space Res. **15** (1974) 651.
74Gol Golub, L., Krieger, A.S., Silk, J.K., et al.: Astrophys. J. **189** (1974) L93.
74Hub Huber, M.C.E., Foukal, P.V., Noyes, R.W., et al.: Astrophys. J. **194** (1974) L115.
74Ree Reeves, E.M., Foukal, P.V., Huber, M.C.E., et al.: Astrophys. J. **188** (1974) L27.
75Bol Boland, B.C., Dyer, E.P., Firth, J.G., et al.: Mon. Not. R. astr. Soc. **171** (1975) 697.
75Tim Timothy, A.F., Krieger, A.S., Vaiana, G.S.: Sol. Phys. **42** (1975) 135.

76Bru Brueckner, G.E., Bartoe, J.-D.F., Kjeldseth-Moe, O., Van Hoosier, M.E.: Astrophys. J. **209** (1976) 935.
76Cus Cushman, G.W., Rense, W.A.: Astrophys. J. **207** (1976) L61.
76Dos1 Doschek, G.A., Feldman, U., VanHoosier, M.E., Bartoe, J.-D.F.: Astrophys. J. Suppl. Ser. **31** (1976) 417.
76Dos2 Doschek, G.A., Feldman, U., Bohlin, J.D.: Astrophys. J. **205** (1976) L177.
76Fel1 Feldman, U., Doschek, G.A., VanHoosier, M.E., Purcell, J.D.: Astrophys. J. Suppl. Ser. **31** (1976) 445.
76Fel2 Feldman, U., Doschek, G.A., Patterson, N.P.: Astrophys. J. **209** (1976) 270.
76Gab Gabriel, A.H.: Phil. Trans. Roy. Soc. Lond. A. **281** (1976) 339.
77Boh Bohlin, J.D.: Sol. Phys. **51** (1977) 377.
77Chi Chiuderi-Drago, F., Avignon, Y., Thomas, R.J.: Sol. Phys. **51** (1977) 143.
77Cus Cushman, G.W., Rense, W.A.: Astrophys. J. **211** (1977) L57.
77Kje Kjeldseth Moe, O., Nicolas, K.R.: Astrophys. J. **211** (1977) 579.
78Boh Bohlin, J.D., Sheeley, N.R., Jr.: Sol. Phys. **56** (1978) 125.
78Fou Foukal, P.V.: Astrophys. J. **223** (1978) 1046.
78She Sheeley, N.R., Jr.: Sol. Phys. **58** (1978) 405.
79She Sheeley, N.R., Jr., Golub, L.: Sol. Phys. **63** (1979) 119.
80Koh Kohl, J.L., Weiser, H., Withbroe, G.L., et al.: Astrophys. J. **241** (1980) L117.
81Der Dere, K.P., Bartoe, J.-D.F., Brueckner, G.E., et al.: Astrophys. J. **249** (1981) 333.
81Hab Habbal, S.R., Withbroe, G.L.: Sol. Phys. **69** (1981) 77.
82Rot Rottman, G.J., Orrall, F.Q., Klimchuk, J.A.: Astrophys. J. **260** (1982) 326.
82Wit Withbroe, G.L., Kohl, J.L., Weiser, H., Munro, R.H.: Space Sci. Rev. **33** (1982) 17.
83Bru Brueckner, G.E., Bartoe, J.-D.F.: Astrophys. J. **272** (1983) 329.
83Owo Owocki, S.P., Scudder, J.D.: Astrophys. J. **270** (1983) 758.
86Dow Dowdy, J.F., Rabin D., Moore R.L.: Sol. Phys. **105** (1986) 35.
86Sah Sahal-Bréchot, S., Malinovsky, M., Bommier, V.: Astron. Astrophys. **168** (1986) 284.
86San Sandlin, G.D., Bartoe, J.-D.F., Brueckner, G.E., et al.: Astrophys. J. Suppl. Ser. **61** (1986) 801.
89Der Dere, K.P., Bartoe, J.-D.F., Brueckner, G.E., Recely, F.: Astrophys. J. **345** (1989) L95.
89Nic Nicolet, M.: Planet. Space Sci. **37** (1989) 1249.
90Gol Golub, L., Herant, M., Kalata, K., et al.: Nature **344** (1990) 842.
90Has Hassler, D.M., Rottman, G.J., Shoub, E.C., Holzer, T.E.: Astrophys. J. **348** (1990) L77.
91Der Dere, K.P., Bartoe, J.-D.F., Brueckner, G.E., et al.: J. Geophys. Res. **96** (1991) 9399.
91Neu Neugebauer, M.: Science **252** (1991) 404.
92Axf Axford, W.I., McKenzie, J.F.: Solar Wind Seven (E. Marsch and R. Schwenn, eds.) Oxford: Pergamon Press (1992) p. 1.
92Hab Habbal, S.R.: Ann. Geophys. **10** (1992) 34.
93Bre Brekke, P.: Astrophys. J. **408** (1993) 735.
93Der Dere, K.P., Mason, H.E.: Sol. Phys. **144** (1993) 217.
93Web Webb, D.F., Martin, S.F., Moses, D., Harvey, J.W.: Sol. Phys. **144** (1993) 15.
94Bre Brekke, P.: Space Sci. Rev. **70** (1994) 97.
94Der Dere, K.P.: Adv. Space Res. **14** (1994) 13.
94Kje Kjeldseth-Moe, O., Cheng, C.C.: Space Sci. Rev. **70** (1994) 85.
94Mos Moses, D., Cook, J.W., Bartoe, J.-D.F., et al.: Astrophys. J. **430** (1994) 913.
95Fis Fisher, R., Guhathakurta, M.: Astrophys. J. **447** (1995) L139.
95Koh Kohl, J.L., Gardner, L.D., Strachan, L., et al.: Space Sci. Rev. **72** (1995) 29.
96Kan Kano, R., Tsuneta, S.: PASJ, **48** (1996) 535.

96Koh Kohl, J.L., Strachan, L., Gardner, L.D.: Astrophys. J. **465** (1996) L141.
97Ant Antonucci, E., Noci, G., Kohl, J.L., et al.: ASP Conf. Ser. **118** (1997) 273.
97Bre Brekke, P., Hassler, D.M., Wilhelm, K.: Sol. Phys. **175** (1997) 349.
97Cor Corti, G., Poletto, G., Romoli, M., et al.: Proc. of the Fifth SOHO Workshop, ESA SP-**404** (1997) 289.
97DeF DeForest, C.E., Hoeksema, J.T., Gurman, J.B., et al.: Sol. Phys. **175** (1997) 393.
97Dos Doschek, G.A., Warren, H.P., Laming, J.M., et al.: Astrophys. J. **482** (1997) L109.
97Flu Fludra, A., Brekke, P., Harrison, R.A., et al.: Sol. Phys. **175** (1997) 487.
97Hab Habbal, S.R., Woo, R., Fineschi, S., et al.: Astrophys. J. **489** (1997) L103.
97Har Harrison, R.A.: Sol. Phys. **175** (1997) 467.
97Has Hassler, D.M., Wilhelm, K., Lemaire, P., Schühle, U.: Sol. Phys. **175** (1997) 375.
97Inn Innes, D.E., Inhester, B., Axford, W.I., Wilhelm, K.: Nature **386** (1997) 811.
97Koh Kohl, J.L., Noci, G., Anonucci, E., et al.: Sol. Phys. **170** (1997) 613.
97Koy Ko, Y.-K., Fisk, L.A., Geiss, J., et al.: Sol. Phys. **171** (1997) 345.
97Lem Lemaire, P., Wilhelm, K., Curdt, W., et al.: Sol. Phys. **170** (1997) 105.
97Mos Moses, D., Clette, F., Delaboudinière, J.-P., et al.: Sol. Phys. **175** (1997) 571.
97Ray Raymond, J.C., Kohl, J.L., Noci, G., et al.: Sol. Phys. **175** (1997) 645.
97See Seely, J.F., Feldman, U., Schühle, U., et al.: Astrophys. J. **484** (1997) L87.
97She Sheeley, N.R., Jr., Wang, Y.-M., Hawley, S.H., et al.: Astrophys. J. **484** (1997) 472.
97Wan Wang, Y.-M., Sheeley, N.R., Jr., Dere, K.P., et al.: Astrophys. J. **484** (1997) L75.
97War1 Warren, H.P., Mariska, J.T., Wilhelm, K., Lemaire, P.: Astrophys. J. **484** (1997) L91.
97War2 Warren, H.P., Mariska, J.T., Wilhelm, K.: Astrophys. J. **490** (1997) L187.
97Woc Woch, J., Axford, W.I., Mall, U., et al.: Geophys. Res. Lett. **24** (1997) 2885.
97Woo Woo, R., Martin, J.: Geophys. Res. Lett. **24** (1997) 2535.
98Cha1 Chae, J., Schühle, U., Lemaire, P.: Astrophys. J. **505** (1998) 957.
98Cha2 Chae, J., Wang, H., Lee, C.-Y., et al.: Astrophys. J. **497** (1998) L109.
98Cha3 Chae, J., Wang, H., Lee, C.-Y., et al.: Astrophys. J. **504** (1998) L123.
98Dav David, C., Gabriel, A.H., Bely-Dubau, F., et al.: Astron. Astrophys. **336** (1998) L90.
98deB de Boer, C.R., Stellmacher, G., Wiehr, E.: Astron. Astrophys. **334** (1998) 280.
98DeF DeForest, C.E., Gurman, J.B.: Astrophys. J. **501** (1998) L217.
98Dos Doschek, G.A., Feldman, U., Laming, et al.: Astrophys. J. **507** (1998) 991.
98Fel Feldman, U.: Space Sci. Rev. **85** (1998) 227.
98Gal Gallagher, P.T., Phillips, K.J.H., Harra-Murnion, L.K., Keenan, F.P.: Astron. Astrophys. **335** (1998) 733.
98McC McComas, D.J., Bame, S.J., Barraclough, B.L., et al.: Geophys. Res. Lett. **25** (1998) 1.
98Tuc Tu, C.-Y., Marsch, E., Wilhelm, K., Curdt, W.: Astrophys. J. **503** (1998) 475.
98Wan Wang, Y.-M.: Astrophys. J. **501** (1998) L145.
98Wil1 Wilhelm, K., Lemaire, P., Dammasch, I.E., et al.: Astron. Astrophys. **334** (1998) 685.
98Wil2 Wilhelm, K., Marsch, E., Dviwedi, B.N., et al.: Astrophys. J. **500** (1998) 1023.
99Bre Brekke, P.: Sol. Phys. **190** (1999) 379.
99Cra1 Cranmer, S.R., Field, G.B., Kohl, J.L.: Astrophys. J. **518** (1999) 937.
99Cra2 Cranmer, S.R., Kohl, J.L., Noci, G., et al.: Astrophys. J. **511** (1999) 481.
99Dam Dammasch, I.E., Wilhelm, K., Curdt, W., Hassler, D.M.: Astron. Astrophys. **346** (1999) 285.
99Ess Esser, R., Fineschi, S., Dobrzycka, D., et al.: Astrophys. J. **510** (1999) L63.
99Fel Feldman, U., Doschek, G.A., Schühle, U., Wilhelm, K.: Astrophys. J. **518** (1999) 500.
99Flu Fludra, A., Del Zanna, G., Alexander, D., Bromage, B.J.I.: J. Geophys. Res. **104** (1999) 9709.

99Fon Fontenla, J., White, O.R., Fox, P.A. et al.: Astrophys. J. **518** (1999) 480.
99Gal Gallagher, P.T., Phillips, K.J.H., Harra-Murnion, L.K., et al.: Astron. Astrophys. **348** (1999) 251.
99Gol Golub, L., Bookbinder, J., DeLuca, E., et al.: Phys. Plasma **6** (1999) 2205.
99Gri Griffiths, N.W., Fisher, G.H., Woods, D.T., Siegmund, O.H.W.: Astrophys. J. **512** (1999) 992.
99Har Harrison, R.A., Lang, J., Brooks, D.H., Innes, D.E.: Astron. Astrophys. **351** (1999) 1115.
99Has Hassler, D.M., Dammasch, I.E., Lemaire, P., et al.: Science **283** (1999) 810.
99Koh Kohl, J.L., Esser, R., Cranmer, S.R., et al.: Astrophys. J. **510** (1999) L59.
99Len Lenz, D.D., DeLuca, E.E., Golub, L., et al.: Astrophys. J. **517** (1999) L155.
99Lit Lites, B.W., Card, G., Elmore, D.F., et al.: Sol. Phys. **190** (1999) 185.
99Mar Marsch, E., Tu, C.-Y., Heinzel, P., et al.: Astron. Astrophys. **347** (1999) 676.
99Ofm Ofman, L., Nakariakov, V.M., DeForest, C.E.: Astrophys. J. **514** (1999) 441.
99Pet1 Peter, H.: Astrophys. J. **516** (1999) 490.
99Pet2 Peter, H., Judge, P.: Astrophys. J. **522** (1999) 1148.
99Wil Wilhelm, K.: Astrophys. Space Sci. **264** (1999) 43.
99You Young, P.R., Klimchuk, J.A., Mason H.E.: Astron. Astrophys. **350** (1999) 286.
99Zha Zhao, X.P, Hoeksema, J.T., Scherrer, P.H.: J. Geophys. Res. **104** (1999) 9735.
00Ale Aletti, V., Velli, M., Bocchialini, K., et al.: Astrophys. J. **544** (2000) 550.
00Asc Aschwanden, M.J., Tarbell, T.D., Nightingale, R.W., et al.: Astrophys. J. **535** (2000) 1047.
00Ban1 Banerjee, D., O'Shea, E., Doyle, J.G.: Sol. Phys. **196** (2000) 63.
00Ban2 Banerjee, D., Teriaca, L., Doyle, J.G., Lemaire, P.: Sol. Phys. **194** (2000) 43.
00Cha Chae, J., Wang, H., Goode, P.R., et al.: Astrophys. J. **528** (2000) L119.
00Dos Doschek, G.A., Feldman, U.: Astrophys. J. **529** (2000) 599.
00Fel Feldman, U., Dammasch, I.E., Wilhelm, K.: Space Sci. Rev. **93** (2000) 411.
00Gio Giordano, S., Antonucci, E., Noci, G., et al.: Astrophys. J. **531** (2000) L79.
00Lan Landi, E., Mason, H.E., Lemaire, P., Landini, M.: Astron. Astrophys. **357** (2000) 743.
00Par1 Parenti, S., Bromage, B.J.I., Poletto, G., et al.: Astron. Astrophys. **363** (2000) 800.
00Par2 Parnell, C.E., Jupp, P.E.: Astrophys. J. **529** (2000) 554.
00Pat Patsourakos, S., Vial, J.-C.: Astron. Astrophys. **359** (2000) L1.
00Rea Reale, F., Peres, G.: Astrophys. J. **528** (2000) L45.
00Syk Sýkora, J., Badalyan, O.G., Obridko, V.N.: Adv. Space Res. **29** (2000) 395.
00Wil1 Wilhelm, K.: Astron. Astrophys. **360** (2000) 351.
00Wil2 Wilhelm, K., Dammasch, I.E., Marsch, E., Hassler, D.M.: Astron. Astrophys. **353** (2000) 749.
01Ban Banerjee, D., O'Shea, E., Doyle, J.G., Goossens, M.: Astron. Astrophys. **377** (2001) 691.
01Brk Brković, A., Solanki, S.K., Rüedi, I.: Astron. Astrophys. **373** (2001) 1056.
01DeF DeForest, C.E., Lamy, P.C., Llebaria, A.: Astrophys. J. **560** (2001) 490.
01Inn Innes, D.E.: Astron. Astrophys. **378** (2001) 1067.
01Pet Peter, H.: Astron. Astrophys. **374** (2001) 1108.
01Ter Teriaca, L., Madjarska, M.S., Doyle, J.G.: Sol. Phys. **200** (2001) 91.
01Zha Zhang, J., Dere, K.P., Howard, R.A., et al.: Astrophys. J. **559** (2001) 452.
02Fol Foley, C.R., Patsourakos, S., Culhane, J.L., MacKay, D.: Astron. Astrophys. **381** (2002) 1049.
02Fra Frazin, R.A., Janzen, P.: Astrophys. J. **570** (2002) 408.
02Har Harrison, R.A., Hood, A.W., Pike, C.D.: Astron. Astrophys. **392** (2002) 319.
02Pat Patsourakos, S., Habbal, S.R., Hu, Y.Q.: Astrophys. J. **581** (2002) L125.

02Rao Raouafi, N.-E., Sahal-Bréchot, S., Lemaire, P., Bommier, V.: Astron. Astrophys. **390** (2002) 691.
02Str Strachan, L., Suleiman, R., Panasyuk, A.V., et al.: Astrophys. J. **571** (2002) 1008.
02Ter Teriaca, L., Falchi, A., Doyle, J.G., et al.: Proc. of 10th European Solar Physics Meeting, ESA SP-**506** (2002) 777.
02War Warren, H.P., Warshall, A.D.: Astrophys. J. **571** (2002) 999.
02Wil1 Wilhelm, K., Inhester, B., Newmark, J.S.: Astron. Astrophys. **382** (2002) 328.
02Wil2 Wilhelm, K., Dammasch, I.E., Xia, L.: Adv. Space Res. **30** (2002) 517.
02Win Winebarger, A.R., Emslie, A.G., Mariska, J.T., Warren, H.P.: Astrophys. J. **565** (2002) 1298.
03Brk Brković, A., Peter, H., Solanki, S.K.: Astron. Astrophys. **403** (2003) 725.
03Che Chen, Y., Esser, R., Hu, Y.Q.: Astrophys. J. **582** (2003) 467.
03Del Del Zanna, G., Bromage, B.J.I., Mason, H.E.: Astron. Astrophys. **398** (2003) 743.
03DeP De Pontieu, B., Tarbell, T., Erdélyi, R.: Astrophys. J. **590** (2003) 502.
03Fra Frazin, R.A., Cranmer, S.R., Kohl, J.L.: Astrophys. J. **597** (2003) 1145.
03Gab Gabriel, A.H., Bely-Dubau, F., Lemaire, P.: Astrophys. J. **589** (2003) 623.
03Har Harrison, R.A., Harra, L.K., Brković, A., Parnell, C.E.: Astron. Astrophys. **409** (2003) 755.
03Hin Hinkle, K., Wallace, L., Livingston, W., et al.: Proc. of the 12th Cambridge Workshop on Cool Stars, Stellar Systems, and the Sun (A. Brown, G.M. Harper, and T.R. Ayres, eds.) University of Colorado (2003) p. 851.
03Mad Madjarska, M.S., Doyle, J.G., Teriaca, L., Banerjee, D.: Astron. Astrophys. **398** (2003) 775.
03Pet Peter, H., Brković, A.: Astron. Astrophys. **403** (2003) 287.
03Ter Teriaca, L., Poletto, G., Romoli, M., Biesecker, D.: Astrophys. J. **588** (2003) 566.
04Cir Cirigliano, D., Vial, J.-C., Rovira, M.: Sol. Phys. **223** (2004) 95.
04Kre Kretzschmar, M., Lilensten, J., Aboudarham, J.: Astron. Astrophys. **419** (2004) 345.
04Mir Miralles, M.P., Cranmer, S.R., Kohl, J.L.: Adv. Space Res. **33** (2004) 696.
04Pop Popescu, M.D., Doyle, J.G., Xia, L.D.: Astron. Astrophys. **421** (2004) 339.
04Rao Raouafi, N.-E., Solanki, S.K.: Astron. Astrophys. **427** (2004) 725.
04Ter Teriaca, L., Banerjee, D., Falchi, A., et al.: Astron. Astrophys. **427** (2004) 1065.
04Wie Wiegelmann, T., Solanki, S.K.: Sol. Phys. **225** (2004) 227.
04Wil Wilhelm, K., Dwivedi, B.N., Marsch, E., Feldman, U.: Space Sci. Rev. **111** (2004) 415.
04Xia Xia, L., Marsch, E., Wilhelm, K.: Astron. Astrophys. **424** (2004) 1025.
05Aio Aiouaz, T., Peter, H., Lemaire, P.: Astron. Astrophys. **435** (2005) 713.
05Aki Akiyama, S., Doschek, G.A., Mariska, J.T.: Astrophys. J. **623** (2005) 540.
05Ant Antonucci, E., Abbo, L., Dodero, M.A.: Astron. Astrophys. **435** (2005) 699.
05Lan Lanzafame, A.C., Brooks, D.H., Lang, J.: Astron. Astrophys. **432** (2005) 1063.
05Men Mendoza-Torres, J.E., Torres-Papaqui, J.P., Wilhelm, K.: Astron. Astrophys. **431** (2005) 339.
05Tuc Tu, C.-Y., Zhou, C., Marsch, E., Xia, L.-D., et al.: Science **308** (2005) 519.
05Uga Ugarte-Urra, I., Doyle, J.G., Del Zanna, G.: Astron. Astrophys. **435** (2005) 1169.
05Wie Wiegelmann, T., Xia, L.D., Marsch, E.: Astron. Astrophys. **432** (2005) L1.
05Wil Wilhelm, K., Fludra, A., Teriaca, L., et al.: Astron. Astrophys. **435** (2005) 733.
06Doy Doyle, J.G., Taroyan, Y., Ishak, B., et al.: Astron. Astrophys. **452** (2006) 1075.
06Koh Kohl, J.L., Noci, G., Cranmer, S.R., Raymond, J.C.: Astron. Astrophys. Rev. **13** (2006) 31.
06Mar1 Marsch, E.: Adv. Space Res. **38** (2006) 921.
06Mar2 Marsch, E., Zhou, G.-Q., He, J.-S., Tu, C.-Y.: Astron. Astrophys. **457** (2006) 699.

06Pet Peter, H.: Astron. Astrophys. **449** (2006) 759.
06Uzz Uzzo, M., Strachan, L., Vourlidas, A.: Astrophys. J. **645** (2006) 720.
06Wil Wilhelm, K.: Astron. Astrophys. **455** (2006) 697.
06Zaq Zaqarashvili, T.V., Oliver, R., Ballester, J.L.: Astron. Astrophys. **456** (2006) 13.
07Bro Brosius, J.W., Rabin, D.M., Thomas, R.J.: Astrophys. J. **656** (2007) L41.
07Fel Feldman, U., Widing, K.G.: Space Sci. Rev. DOI: 10.1007/s11214-007-9157-7 (2007).
07Pas Pasachoff, J.M., Rŭsin, V., Druckmüller, M., Saniga, M.: Astrophys. J. **665** (2007) 824.